Effects of natural killer cell-conditioned medium on UVB-induced photoaging in human keratinocytes and a human reconstructed skin model

JUNG OK LEE[1*], JUNG MIN LEE[1,2*], YUJIN KIM[1], A YEON PARK[1], DAEWON YOON[1,2], SU YOUNG KIM[1,2], JIHYE HEO[1,2], SEUNGRYEL HAN[3], HYUNGJIN NAM[3], HYE JIN SHIN[3], KYEONGSOO JEONG[4], MINJU IM[4] and BEOM JOON KIM[1,2]

[1]Department of Dermatology, College of Medicine, Chung-Ang University, Seoul 06974, Republic of Korea; [2]Department of Medicine, Graduate School, Chung-Ang University, Seoul 06973, Republic of Korea; [3]GC Cell Co., Ltd., Yongin, Seoul 16924, Republic of Korea; [4]Green Cross Wellbeing Co., Ltd., Yongin, Seoul 16950, Republic of Korea

Received September 4, 2024; Accepted February 10, 2025

DOI: 10.3892/mmr.2025.13488

Abstract. Natural killer (NK) cells produce various cytokines, including interleukin (IL)-1β, IL-6, IL-10, IL-12, interferon γ, tumor necrosis factor α and transforming growth factor β, which are critical in modulating immune responses. NK cell-conditioned medium (NK-CdM), rich in cytokines, has potential applications in therapy and healing. The present study aimed to investigate the protective effect of NK-CdM against ultraviolet B (UVB)-mediated photoaging using *in vitro* and *ex vivo* models. In human keratinocyte cell line (HaCaT cells), NK-CdM mitigated UVB-induced cytotoxicity and suppressed the production of reactive oxygen species. NK-CdM enhanced the mRNA expression levels of superoxide dismutase 1 (SOD1) and catalase (CAT) and inhibited the reduction in SOD1 and CAT expression levels caused by UVB irradiation. Furthermore, NK-CdM inhibited the UVB-mediated nuclear translocation of nuclear factor erythroid 2-related factor 2. NK-CdM also prevented UVB-induced downregulation of filaggrin and involucrin and attenuated the UVB-induced reduction in hyaluronan synthase (HAS)1, HAS2, HAS3, aquaporin-3 and hyaluronan levels. Notably, NK-CdM upregulated the expression of elongation of very long chain fatty acids (ELOVL) enzymes, including ELOVL1, ELOVL5 and ELOVL6, as well as ceramide synthases (CerS), specifically CerS2 and CerS3. Furthermore, NK-CdM inhibited the UVB-induced reduction in the levels of these proteins. Overall, these findings suggested that NK-CdM has the potential to prevent UVB-mediated photoaging and promote skin health.

Correspondence to: Professor Beom Joon Kim, Department of Dermatology, College of Medicine, Chung-Ang University, 102 Heukseok-ro, Dongjak-gu, Seoul 06974, Republic of Korea
E-mail: beomjoon74@gmail.com

*Contributed equally

Key words: natural killer cell, natural killer cell-conditioned medium, reactive oxygen species, ultraviolet B, hyaluronan synthase, nuclear factor erythroid 2-related factor 2

Introduction

The skin is the largest organ in the body and plays a crucial role in protecting the internal organs from various external threats (1). It is continuously exposed to various factors, including pollutants, smoking, diet, heat and ultraviolet radiation (UVR) (2). It is primarily composed of two main layers: the epidermis and the dermis, each with distinct structural and physiological characteristics (3). The epidermis, which is the outermost layer, is directly exposed to the environment and functions primarily as a protective barrier against external agents (4). It is primarily composed of keratinocytes, constituting 90-95% of skin cells, which are essential for maintaining skin hydration and barrier function (5).

Skin aging is generally categorized into chronological aging and UVR-induced photoaging (6). Photoaging is the most significant contributor to skin damage. Long-term exposure to UVR leads to wrinkles, uneven pigmentation, skin dryness and decreased dermal and epidermal thickness (7). UVR can be classified into three types based on wavelength: UVA (320-400 nm), UVB (280-320 nm) and UVC (100-280 nm) (8). Among them, the majority of UVC and some UVB are absorbed by the ozone layer (9). The rest of UVB penetrates the skin epidermis, while UVA invades the dermis, breaking down the extracellular matrix (10). Epidermal cells exposed to UVB exhibit increased levels of reactive oxygen species (ROS). Under physiological conditions, ROS function as essential second messengers in various cellular processes, including cell signaling and immune responses. However, excessive production of ROS induces oxidative stress and DNA damage, contributing to the development of pathological conditions, as well as premature aging and photoaging (11,12).

Maintaining a balance between ROS production and antioxidant defense mechanisms is crucial for cellular health. Cells

possess an antioxidant defense system in the cytoplasm and cellular organelles, comprising enzymatic and non-enzymatic antioxidants (13). Enzymatic antioxidants include superoxide dismutase (SOD), catalase (CAT) and glutathione peroxidase (GPx) and glutathione reductase (GR). Non-enzymatic antioxidants include glutathione, coenzyme Q10 and vitamins C and E. Among them, SOD, CAT and GPx are crucial players for the first line antioxidant system (14). Nuclear factor erythroid 2-related factor 2 (Nrf2) serves as the transcriptional master regulator of a multitude of antioxidant enzymes involved in the detoxification and elimination of oxidative stress genes, such as SOD and CAT (15).

Natural killer (NK) cells, constituting 10-15% of human peripheral blood lymphocytes (16), possess the unique ability to eliminate target cells without the need for major histocompatibility complex restriction. NK cells secrete a diverse array of cytokines that are pivotal in eradicating pathogens and infected cells, as well as in modulating the immune response (17). The cytokines produced by NK cells include interleukin (IL)-1β, IL-6, IL-10, IL-12, tumor necrosis factor α, transforming growth factor β, interferon gamma interferon γ, IL-15 and IL-18 (18). Consequently, NK cell-conditioned medium (NK-CdM), enriched with bioactive cytokines, has demonstrated promising potential across various applications, including immunotherapy, cancer treatment, antiviral, antibacterial and antifungal activities, as well as wound healing (19). Furthermore, previous studies have highlighted the wrinkle-preventive effects of NK-CdM on the dermis of UVB-exposed skin (20). However, the effect of NK-CdM on the epidermal skin barrier following UVB exposure remains unexplored to date. Therefore, the present study aimed to investigate the effects of NK-CdM on the epidermal skin barrier.

Materials and methods

Culture of NK cells and conditioned media preparation. NK-CdM was manufactured with some modifications referring to the conditions described previously (21). Peripheral blood mononuclear cells (PBMCs) were collected from healthy donors (n=3; 2 males and 1 female; average age=36.6) via lymph apheresis for 2-4 batch productions in February 2019 at Seoul National University Hospital (Seoul, Korea; Institutional Review Board approval no. H-1811-023-985). CD3+ T cells in PBMCs were depleted via a magnetic cell sorting system. NK cells present in the CD3-depleted PBMCs were enriched and expanded using irradiated feeder cells and culture medium for ~3 weeks. Feeder cells included genetically engineered T cell lines and the culture medium was Cellgro SCGM medium (CellGenix GmbH) containing human plasma and IL-2. When NK cell cultivation was completed, NK-CdM was harvested using a continuous centrifugation system at 400 x g for 3 min at 4˚C to remove NK cells. NK cell concentration at harvesting NK-CDM was $0.5x10^6$-$3x10^6$ cells/ml. NK-CdM collection and production were performed at GC Cell. The characteristics of NK-CdM following cultivation are summarized in Table I.

Table I. Characterization of the NK-CdM following cultivation.

Characteristic	Value
Cell viability at harvest, %	93
Cell density at harvest, $x10^6$ cell/ml	2.45
Population doubling level	12.98
Cytotoxicity (E:T=10:1, Specific lysis), %	75.9
Identity, %	
$CD3^-CD56^+$	97.9
$CD56^+CD16^+$	95.1
Purity, %	
$CD3^+$	0.0
$CD14^+$	0.0
$CD19^+$	0.0

NK-CdM, NK cell-conditioned medium.

Cell culture and treatment. The human keratinocyte cell line, HaCaT (CLS; cat. no. 300493; Cell Lines Service GmbH), was maintained in Dulbecco's Modified Eagle's Medium (DMEM; Welgene, Inc.) containing 10% fetal bovine serum (FBS; Hyclone; Cytiva) and 1% penicillin/streptomycin at 37˚C with 5% CO_2. The cells were pretreated with 1, 3 or 10% NK-CdM. Following incubation for 3 or 6 h, the culture medium was replaced with 0.5 ml of Dulbecco's phosphate-buffered saline (DPBS; Welgene, Inc.). Subsequently, the cells were exposed to UVB (30 mJ/cm^2) and then treated with NK-CdM.

Cell viability assay. Cytotoxicity of NK-CdM was investigated using a WST-8 assay in HaCaT cells. Cells were seeded into 96-well plates at a density of 5,000 cells per well. Cells were treated with 0, 1, 3, 10, 30 or 100% NK-CdM for 24 h; 0, 5, 10, 15, 20, 25 or 30% NK-CdM for 24 h; or exposed to 30 mJ/cm^2 UVB followed by treatment with 0, 1, 3 or 10% NK-CdM and incubation for 24 h. Additionally, the cells were pretreated with 1, 3 or 10% NK-CdM for 6 h before being exposed to UVB. Cell viability was analyzed using a WST-8 assay at 450 nm using a microplate spectrophotometer (SpectraMax 340; Molecular Devices, LLC).

Intracellular ROS measurement. Intracellular ROS levels were measured using the Cellular ROS Detection Assay Kit (cat. no. ab1183851; Abcam). Fluorescence images were observed using a fluorescence microscope (DMi8; Leica Microsystems GmbH) and fluorescence absorbance was measured at 485 and 535 nm using a spectrophotometer (SpectraMax 340; Molecular Devices, LLC).

Reverse transcription-quantitative (RT-q) PCR. HaCaT cells were seeded into 6-well plates at a density of $3x10^4$ cells per well. The cells were treated with 0, 1, 3 or 10% NK-CdM for 3 h; or exposed to 30 mJ/cm^2 UVB followed by treatment with 0, 1, 3 or 10% NK-CdM and incubation for 1 or 3 h. Total RNA from HaCaT cells was extracted using TRIzol® (Invitrogen; Thermo Fisher Scientific, Inc.) according to the manufacturer's instructions. Additionally, cDNA was synthesized from 1 μg of purified RNA via reverse transcription with oligo-dT primers using a PrimeScript RT Master Mix (Takara Bio, Inc.) according to the manufacturer's instructions. Using qPCR

Table II. Primer sequences used for quantification of gene expression.

Gene	Primer sequence (5'→ 3')	
Human superoxide dismutase 1	Forward	CGACAGAAGGAAAGTAATG
	Reverse	TGGATAGAGGATTAAAGTGAG
Human catalase	Forward	CGTGCTGAATGAGGAACAGA
	Reverse	AGTCAGGGTGGACCTCAGTG
Human filaggrin	Forward	AGGCTCCTTCAGGCTACATTC
	Reverse	CAGGAGAGTAGACATCTTTTGGCA
Human involucrin	Forward	TGCCTGAGCAAGAATGTGAG
	Reverse	AGCTGCTGATCCCTTTGTGT
Human hyaluronan synthase 1	Forward	CAAGATTCTTCAGTCTGGAC
	Reverse	TAAGAACGAGGAGAAAGCAG
Human hyaluronan synthase 2	Forward	ATTACCCAGTCCTGGCTTCG
	Reverse	CCTGTGGAAGACTCAGCAGAA
Human hyaluronan synthase 3	Forward	CTTAAGGGTTGCTTGCTTGC
	Reverse	GTTCGTGGGAGATGAAGGAA
Human aquaporin3	Forward	AGACAGCCCCTTCAGGATTT
	Reverse	TCCCTTGCCCTGAATATCTG
Human elongation of very long chain fatty acids 1	Forward	AATGGGCTCTTTCCATGCCA
	Reverse	GGGAGATGTGCAGTGAGACC
Human elongation of very long chain fatty acids 5	Forward	TGTGATGAACTGGGTCCCCTG
	Reverse	CCAGAGGTATGGACGCATGG
Human elongation of very long chain fatty acids 6	Forward	CCTGTCAGCAAATTCTGGGC
	Reverse	ATGTGGTGATACCAGTGCAGG
Human ceramide synthase2	Forward	ATCGTCTTCGCCATTGTTTT
	Reverse	GGCAGGATAGAGCTCCAGTG
Human ceramide synthase3	Forward	CCAGGCTGAAGAAATTCCAG
	Reverse	AACGCAATTCCAGCAACAGT
Human serine-palmitoyl transferase 2	Forward	AGCCGCCAAAGTCCTTGAG
	Reverse	CTTGTCCAGGTTTCCAATTTCC
Human sphingomyelin synthase 2	Forward	CACCCAGTGGCTGTTTCTGA
	Reverse	TGCATTCCAGGCACAGGTAGA
Human acid sphingomyelinase	Forward	TGGCTCTATGAAGCGATGG
	Reverse	AGGCCGATGTAGGTAGTTGC
Human peroxisome proliferator-activated receptor-α	Forward	CCATCGGCGAGGATAGTTCTG
	Reverse	TCTACATTCGATGTTCAATGCTCCA
Human peroxisome proliferator-activated receptor-γ	Forward	TGGAATTAGATGACAGCGACTTGG
	Reverse	CTGGAGCAGCTTGGCAAACA
Human β-actin	Forward	AGCGAGCATCCCCCAAAGTT
	Reverse	GGGCACGAAGGCTCATCATT

PreMIX SYBR Green (Enzynomics), qPCR was performed on a CFX96 thermocycler (Bio-Rad Laboratories, Inc.). The thermocycling program was as follows: 95˚C for 10 min, followed by 40 cycles at 95˚C for 10 sec, 60˚C for 15 sec and 72˚C for 15 sec. At least three separate biological replicates were conducted for the RT-qPCR. Analysis of relative gene expression data using real-time quantitative PCR and the $2^{-\Delta\Delta Cq}$ method (22), and then normalized to β-actin expression. Table II contains a list of the primers used in the qPCR.

Western blotting. HaCaT cells were seeded into 6-well plates at a density of $3x10^4$ cells per well. HaCaT cells were pretreated with NK-CdM and NAC (10 mM) for 3 h and then exposed to UVB (30 mJ/cm^2) irradiation for 3 h or 24 h at 37˚C with 5% CO_2. Additionally, cells were pretreated with 3% NK-CdM for 3 h, exposed to 30 mJ/cm^2 UVB, and subsequently treated with 3% NK-CdM, followed by incubation for 1 or 24 h. RIPA lysis buffer (Thermo Fisher Scientific, Inc.) was used to extract the HaCaT cellular proteins and the Bradford reagent (Millipore Sigma) was used to measure the protein concentration. Then, 15 μg of the protein samples were separated on a 10% sodium dodecyl sulfate polyacrylamide (SDS-PAGE) gel and transferred onto a nitrocellulose membrane (Cytiva). After that, the membranes were blocked with 5% skimmed milk in

Table III. Antibodies used for western blot analysis.

Antibodies	Dilution	Catalogue number	Supplier
Anti-superoxide dismutase 1	1:3,000	sc-101523	Santa Cruz Biotechnology, Inc.
Anti-catalase	1:3,000	sc-271803	Santa Cruz Biotechnology, Inc.
Anti-nuclear factor erythroid 2-related factor 2	1:3,000	sc-81342	Santa Cruz Biotechnology, Inc.
Anti-lamin B	1:5,000	13435	Cell Signaling Technology, Inc.
Anti-filaggrin	1:5,000	PA5-116911	Thermo Fisher Scientific, Inc.
Anti-filaggrin	1:100	GTX37695	GeneTex
Anti-involucrin	1:5,000	ab53112	Abcam
Anti-hyaluronan synthase1	1:5,000	ab198846	Abcam
Anti-hyaluronan synthase2	1:5,000	sc-365263	Santa Cruz Biotechnology, Inc.
Anti-hyaluronan synthase3	1:5,000	sc-365322	Santa Cruz Biotechnology, Inc.
Anti-Aquaporin3	1:5,000	PA5-78811	Thermo Fisher Scientific, Inc.
Anti-matrix metalloproteinase 9	1:5,000	ab38898	Abcam
Anti-p-p38	1:5,000	4511	Cell Signaling Technology, Inc.
Anti-p38	1:5,000	9212	Cell Signaling Technology, Inc.
Anti-p-c-Jun N-terminal kinases	1:5,000	9251	Cell Signaling Technology, Inc.
Anti-c-Jun N-terminal kinases	1:5,000	9252	Cell Signaling Technology, Inc.
Anti-p-extracellular signal-regulated kinase	1:5,000	9101	Cell Signaling Technology, Inc.
Anti-extracellular signal-regulated kinase	1:5,000	9102	Cell Signaling Technology, Inc.
Anti-p-Jun Proto-Oncogene	1:5,000	#3270	Cell Signaling Technology, Inc.
Anti-Jun Proto-Oncogene	1:5,000	#9165	Cell Signaling Technology, Inc.
Anti-p-cellular oncogene fos	1:5,000	#5348	Cell Signaling Technology, Inc.
Anti-cellular oncogene fos	1:5,000	#2250	Cell Signaling Technology, Inc.
Anti-ceramide synthases 3	1:5,000	PA1-12923	Thermo Fisher Scientific, Inc.
Anti-serine-palmitoyl transferase	1:5,000	ab307432	Abcam
Anti-acid sphingomyelinase	1:5,000	PA5-77047	Thermo Fisher Scientific, Inc.
Anti-β-actin	1:10,000	sc-47778	Santa Cruz Biotechnology, Inc.

p-, phosphorylated.

Tris-buffered saline containing 0.1% Tween-20 (TBS-T) at room temperature for 1 h and then incubated overnight at 4˚C with primary antibodies listed in Table III. Following washes, the membranes were incubated with horseradish peroxidase (HRP)-conjugated anti-mouse or anti-rabbit secondary antibodies (Vector Laboratories, Ltd.). Immunodetection was performed using an Amersham ECL kit (Cytiva) according to the manufacturer's instructions. Protein bands were visualized using a ChemiDoc MP Imaging System (Bio-Rad Laboratories, Inc.) and ImageJ v1.8.0 (National Institutes of Health) was used for analysis, normalizing all target proteins to β-actin.

SOD activity measurement. SOD activity was assessed using a colorimetric assay kit (Biomax Ltd.) following the manufacturer's instructions. Cells were treated with 3% NK-CdM or NAC (N-Acetyl cysteine; antioxidant) for 6 h. Following UVB irradiation, the cells were homogenized in cold lysis buffer and absorbance was measured at 450 nm to evaluate SOD activity using a microplate spectrophotometer (SpectraMax 340; Molecular Devices, LLC).

Reconstructed human skin model. Neoderm-ED, a reconstructed human skin model, was purchased from Tego Science. Neoderm-ED was removed from the agar-containing medium and placed into 12-well plates to equilibrate at 37˚C (5% CO_2) for 24 h. Neoderm-ED was pretreated with NK-CdM or D-panthenol (DPA) for 24 h before being exposed to UVB irradiation (30 mJ/cm^2) for 48 h.

Histological observation and immunohistochemistry (IHC). Neoderm-ED was fixed in 10% formalin at room temperature for 24 h, dehydrated in ethanol, cleared with xylene, embedded in paraffin, sectioned into 3-μm-thick slices, and stained with hematoxylin and eosin (H&E). The skin model was subjected to antigen retrieval with Tris-EDTA at 4˚C for 15 min, followed by treatment with BLOXALL blocking solution (Vector Laboratories, Ltd.) at room temperature for 10 min to quench endogenous peroxidase activity. The slides were then incubated with 2.5% normal horse serum (Vector Laboratories, Ltd.) and Filaggrin antibodies (Table III) overnight at 4˚C. Following this, the slides were incubated with HRP using the ImmPRESS® Excel Amplified Polymer Staining Kit (Vector Laboratories, Ltd.) and staining was developed using the 3,3'-diaminobenzidine (DAB) chromogenic substrate kit (Vector Laboratories, Ltd.). Finally, the slides were counterstained with hematoxylin at room temperature for <1 min to identify nuclei. The slides

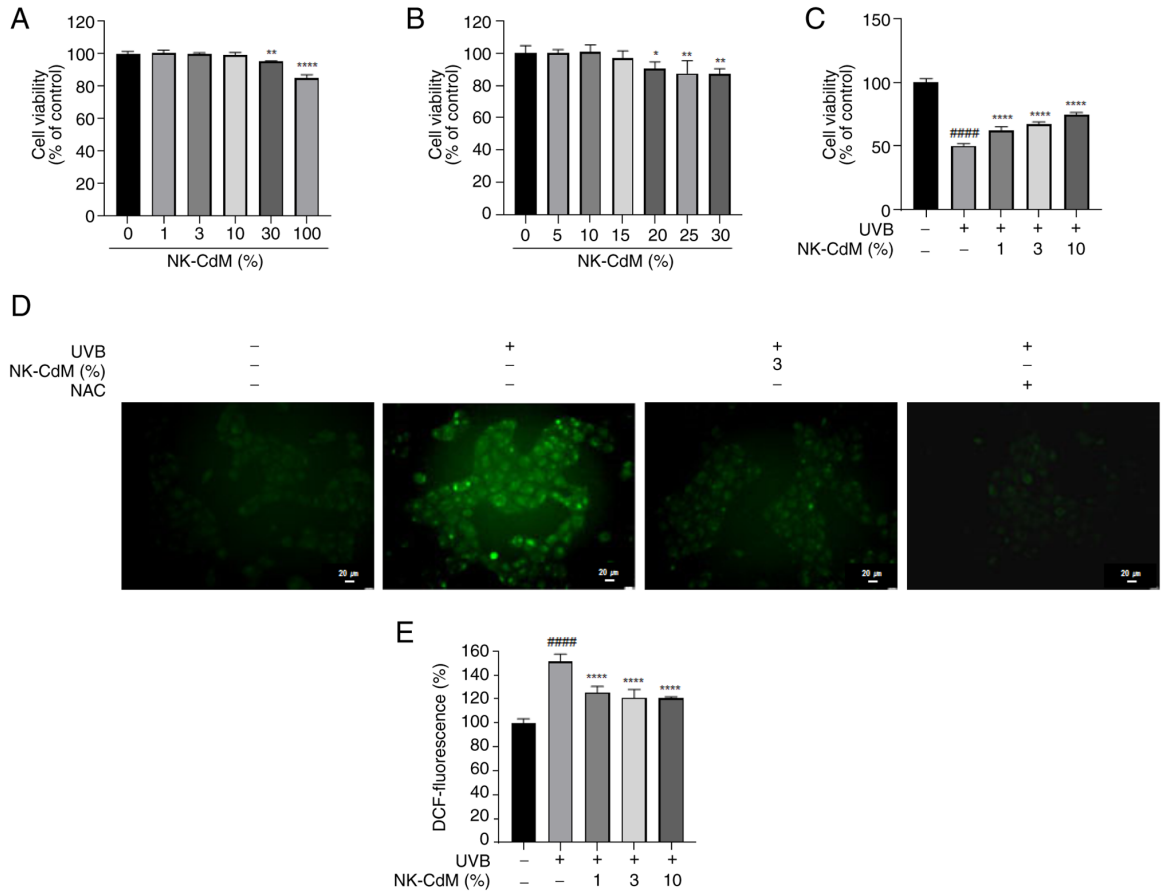

Figure 1. Effect of NK-CdM on cell viability and intracellular ROS levels in HaCaT cells. (A and B) The cell viability of non-UVB-exposed HaCaT cells was determined after incubation with 1-100% NK-CdM for 24 h. (C) The protective effect of NK-CdM (1, 3 and 10%) on cells irradiated with UVB (30 mJ/cm^2). (D and E) HaCaT cells were pretreated with NK-CdM for 3 h and irradiated with UVB (30 mJ/cm^2). Then, the cells were exposed to DCFHDA for 45 min. The images and fluorescence were acquired using a fluorescence microscope and spectrophotometer. Scale bar, 20 μm. The results are expressed as the mean ± standard deviation of three independent experiment. $^{\#\#\#\#}$P<0.0001 vs. the control group (untreated group). *P<0.05, **P<0.01 and ****P<0.0001 vs. the UVB-irradiated group. NK-CdM, NK cell-conditioned medium; ROS, reactive oxygen species; UVB, ultraviolet B; DCFHDA, 2',7'-dichlorofluorescein diacetate.

were cleaned, dried and then mounted with Permount™ mounting medium (Thermo Fisher Scientific, Inc.). The stained slides were observed under a light microscope (DM750; Leica Microsystems GmbH). A slide scanner (Panoramic MIDI; 3DHISTECH Ltd.) was used to capture images of all the stained tissue slides at a magnification of 200x.

Enzyme-linked immunosorbent assay (ELISA). HaCaT cells were seeded into 6-well plates at a density of 500,000 cells per well. The Cells were pretreated with 3% NK-CdM and 1% DPA, positive control, for 9 h, followed by UVB (30 mJ/cm^2) irradiation for 24 h. Following incubation, samples were taken and centrifuged at 3,000 x g for 10 min at 4˚C. The supernatants were then analyzed for HA using an ELISA. The procedure was performed using an ELISA kit (cat. no. DHYAL0; R&D Systems) following the provided instructions.

Statistical analyses. Data were obtained from at least three independent experiments and presented as mean ± standard deviation (SD). Statistical analyses were performed using unpaired one-way analysis of variance followed by a Bonferroni post hoc test on GraphPad Prism 9.0 (Dotmatics). The Bonferroni post hoc test was used among the groups. Data are likely to be sampled from a normally distributed population, as determined using Shapiro-Wilk test (P<0.05). The results were considered significant as follows: $^{\#}$P<0.05, $^{\#\#}$P<0.01, $^{\#\#\#}$P<0.001 and $^{\#\#\#\#}$P<0.0001 vs. the control group (untreated group). *P<0.05, **P<0.01, ***P<0.001 and ****P<0.0001 vs. the UVB-irradiated group. P<0.05 was considered to indicate a statistically significant difference.

Results

NK-CdM protects against UVB-induced cytotoxicity by reducing ROS production. The viability of HaCaT cells was assessed using the WST-8 assay. A viability threshold of ~80% was established to indicate non-toxic conditions. NK-CdM did not exhibit any toxicity at concentrations up to 10%, but cell viability decreased by 15% at a concentration of 100% (Fig. 1A). A more detailed assessment of NK-CdM concentrations ~30% revealed that cell viability showed a slight decrease at 15%, though it was not statistically significant. However, cell viability decreased markedly at 20% NK-CdM (Fig. 1B). Therefore, 10% was selected as the maximum concentration for subsequent experiments with NK-CdM. To evaluate the protective effects of NK-CdM against UVB-induced damage,

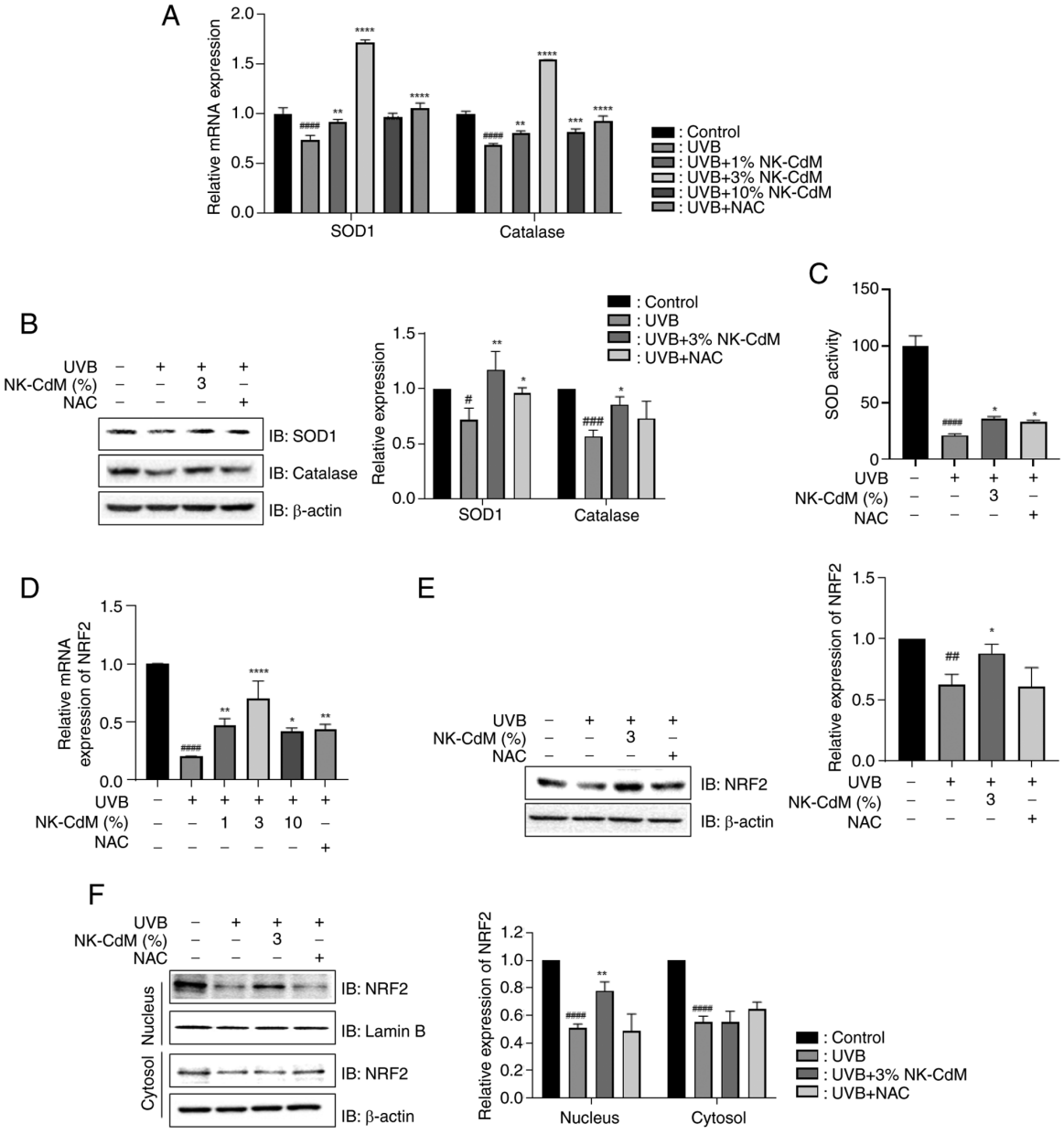

Figure 2. Effect of NK-CdM on UVB-induced oxidative stress in UVB-stimulated HaCaT cells. The mRNA and protein levels in HaCaT cells pretreated with NK-CdM and NAC (10 mM) for 3 h and exposed to UVB (30 mJ/cm^2) irradiation for 3 and 24 h. The (A) mRNA and (B) protein levels of antioxidant enzymes, including SOD1 and CAT. (C) Effect of NK-CdM on SOD activity. The (D) mRNA and (E) protein levels of Nrf2, a key regulator of intracellular antioxidants. (F) Protein expression of Nrf2 in cytoplasm and nucleus fractions. The results are expressed as the mean ± standard deviation of three independent experiment. $^{\#}$P<0.05, $^{\#\#}$P<0.01, $^{\#\#\#}$P<0.001 and $^{\#\#\#\#}$P<0.0001 vs. the control group (untreated group). *P<0.05, **P<0.01, ***P<0.001 and ****P<0.0001 vs. the UVB-irradiated group. NK-CdM, NK cell-conditioned medium; UVB, ultraviolet B; SOD1, superoxide dismutase 1; CAT, catalase; Nrf2, nuclear factor erythroid 2-related factor 2.

HaCaT cells were pretreated with NK-CdM at concentrations of 1, 3 and 10% prior to UVB exposure at a dose of 30 mJ/cm^2. Cell viability increased by 12% (UVB + NK-CdM 1% group), 17% (UVB + NK-CdM 3% group) and 24% (UVB + NK-CdM 10% group) compared with the UVB-only group (Fig. 1C). To determine whether the antioxidant properties of NK-CdM contribute to its protective effects against UVB, intracellular and extracellular ROS production was assessed using the H2DCFDA assay. Furthermore, DCF-DA staining was conducted to measure the ROS levels in the cells. As shown in Fig. 1D, UVB irradiation markedly increased ROS accumulation in the cytoplasm and mitochondria, while pretreatment with NK-CdM alleviated the ROS levels in the cells. In addition, UVB markedly increased ROS production compared with the control, whereas pretreatment with 3% NK-CdM reduced ROS production by 30% relative to the UVB-only group (Fig. 1D and E).

NK-CdM alleviates UVB-induced oxidative stress. Next, the present study investigated the role of NK-CdM in modulating the antioxidant defense system. The mRNA and protein expression levels of SOD1 and CAT were analyzed. As shown in Fig. 2A and B, UVB irradiation decreased the expression of these proteins; however, treatment with

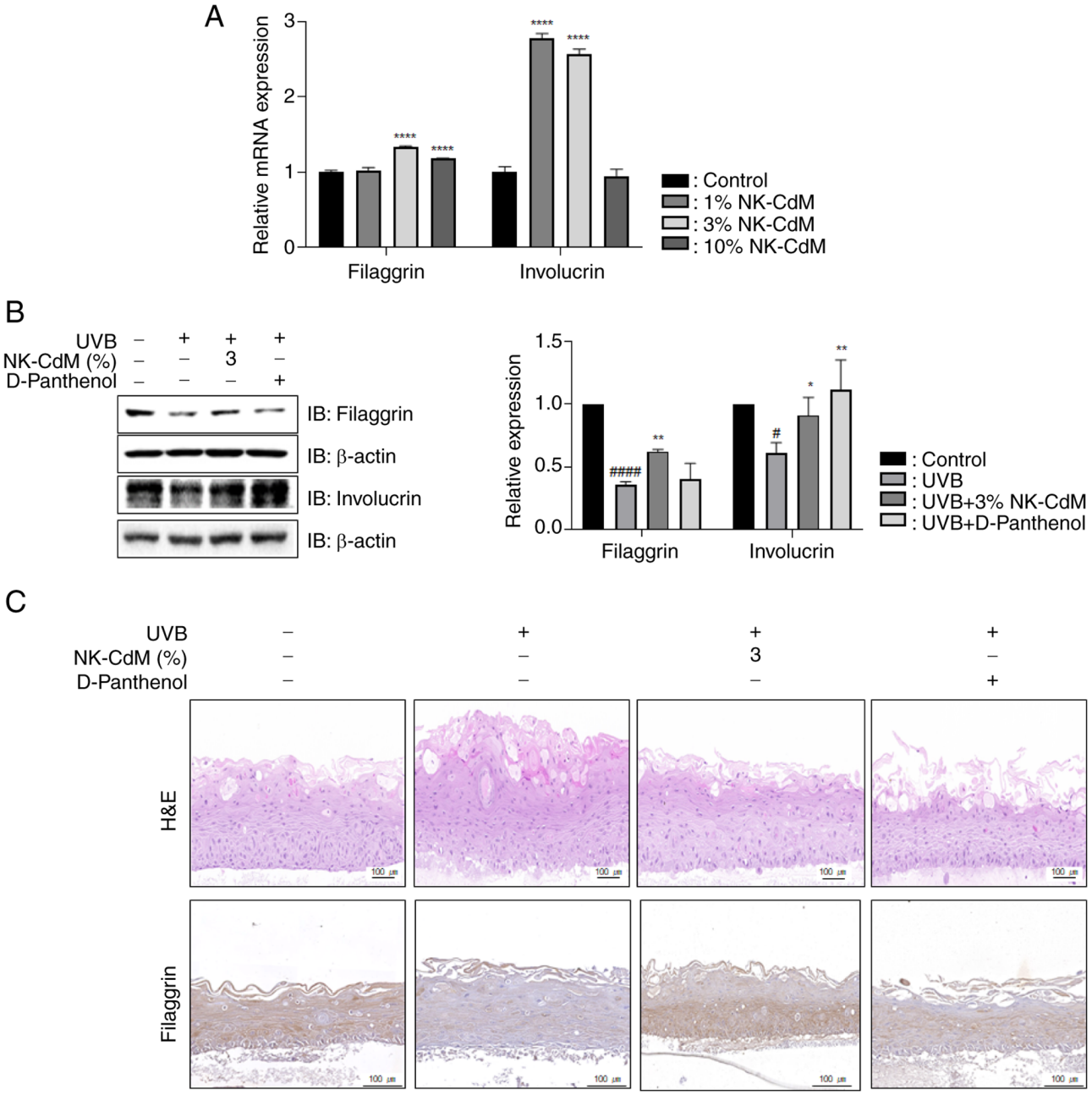

Figure 3. Effect of NK-CdM on skin barrier in UVB-stimulated HaCaT cells and reconstructed human skin model. (A) Direct effect of NK-CdM on the mRNA levels of FLG and IVL. (B) Protein levels of FLG and IVL in UVB-stimulated HaCaT cells (images taken from different gels). (C) Representative images of hematoxylin and eosin staining and histological images of FLG in the reconstructed human skin tissue model. Scale bar, 100 μm. The results are expressed as the mean ± standard deviation of three independent experiment. $^{\#}$P<0.05 and $^{\#\#\#\#}$P<0.0001 vs. the control group (untreated group). *P<0.05, **P<0.01 and ****P<0.0001 vs. the UVB-irradiated group. NK-CdM, NK cell-conditioned medium; UVB, ultraviolet B; FLG, filaggrin; IVL, involucrin.

NK-CdM reversed this effect compared with UVB-treated cells. Similarly, NK-CdM treatment alleviated the UVB-induced reduction in SOD activity (Fig. 2C). Nrf2, a key transcription factor that regulates SOD 1 and CAT genes, was markedly downregulated at both mRNA and protein levels in UVB-irradiated cells. However, NK-CdM attenuated this effect (Fig. 2D and E). Moreover, NK-CdM prevented the UVB-induced decrease in Nrf2 localization to the nucleus (Fig. 2F).

NK-CdM protects the skin barrier by increasing filaggrin (FLG) and involucrin (IVL) expression. To determine the role of NK-CdM in skin barrier function, the present study measured the mRNA expression levels of both FLG and IVL following NK-CdM treatment. NK-CdM increased the expression levels of FLG and IVL (Fig. 3A). As shown in Fig. 3B, the levels of FLG and IVL decreased in the UVB-only group compared with the non-irradiated group. However, the expression levels of FLG and IVL were upregulated in the NK-CdM-treated group compared with the UVB-only group. Additionally, in a three-dimensional (3D) artificial skin model, NK-CdM markedly reduced UVB-induced epidermal hyperplasia (Fig. 3C) and restored FLG expression that had been decreased by UVB irradiation. These results suggest that

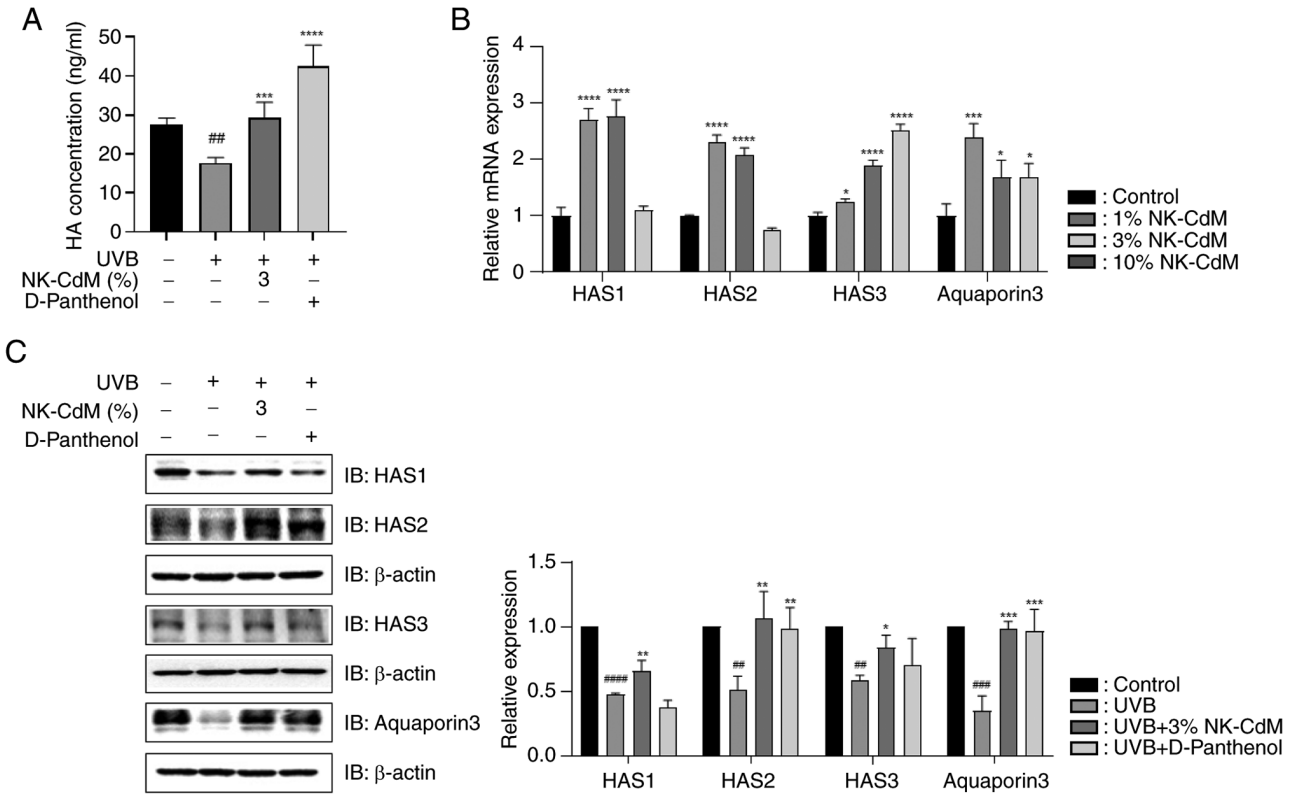

Figure 4. Effect of NK-CdM on skin hydration in UVB-stimulated HaCaT cells. (A) HA expression levels were analyzed using ELISA in HaCaT cells. (B) Direct effect of NK-CdM on the mRNA levels of HAS1, HAS2, HAS3 and AQP3. (C) Protein levels of HAS1, HAS2, HAS3 and AQP3 in UVB-stimulated HaCaT cells. The results are expressed as the mean ± standard deviation of three independent experiment. $^{\#\#}$P<0.01, $^{\#\#\#}$P<0.001 and $^{\#\#\#\#}$P<0.0001 vs. the control group (untreated group). *P<0.05, **P<0.01, ***P<0.001 and ****P<0.0001 vs. the UVB-irradiated group. The western blot results in Figure 4C are images taken from different gels. NK-CdM, NK cell-conditioned medium; UVB, ultraviolet B; ELISA, enzyme-linked immunosorbent assay; HAS, hyaluronan synthase; AQP3, aquaporin 3.

NK-CdM exerts an anti-photoaging effect by enhancing skin barrier function.

NK-CdM attenuates the UVB-induced reduction in the levels of hyaluronan synthase (HAS)1, HAS2, HAS3, aquaporin 3 (AQP3) and hyaluronan (HA). As shown in Fig. 4A, HA production markedly increased by 43% in the UVB + NK-CdM group compared with the UVB-only group. NK-CdM also reversed the UVB-induced reduction in HA production. To further investigate the skin hydration efficacy of NK-CdM, the mRNA levels of HAS1, HAS2, HAS3 and AQP3 were examined. Treatment with 1 and 3% NK-CdM markedly increased the expression levels of HAS1, HAS2, HAS3 and AQP3 (Fig. 4B). Moreover, NK-CdM effectively mitigated UVB-induced reduction in these proteins (Fig. 4C).

NK-CdM inhibits UVB-induced matrix metalloproteinase-9 (MMP-9) expression and mitogen-activated protein kinase (MAPK) phosphorylation. The effect of NK-CdM treatment on MMP-9 expression following UVB irradiation was examined. NK-CdM markedly reduced the UVB-induced MMP-9 production (Fig. 5A). The results revealed that UVB exposure stimulated overall MAPK signaling molecules, but NK-CdM suppressed the phosphorylation of extracellular signal-regulated kinase (ERK), c-Jun N-terminal kinases (JNK) and p38 (Fig. 5B). In addition, UVB-induced phosphorylation of the AP-1 subunits (c-Fos and c-Jun) was markedly suppressed by NK-CdM treatment (Fig. 5C).

NK-CdM increases the mRNA levels of enzymes involved in ceramide (CER) synthesis. To examine the effect of NK-CdM on the expression of enzymes involved in the synthesis of CERs containing long-chain fatty acids (FAs), the mRNA levels of ELOVL isozyme, CER synthase (CerS) isozymes and serine-palmitoyl transferase 2 (SPT2) were assessed. NK-CdM treatment significantly upregulated the mRNA expression of ELOVL1 at a concentration of 1%, ELOVL5 at 3%, and ELOVL6 at 10% (Fig. 6A). Similarly, MK-CdM increased the mRNA expression levels of CerS2, CerS3 and SPT2 across these concentrations (Fig. 6B). Further assessment of CER production in the stratum corneum (SC) was conducted by measuring the expression of sphingomyelin synthase (SMS) and acid sphingomyelinase (ASM). NK-CdM increased the mRNA expression levels of SMS2 and ASM (Fig. 6C). The effect of NK-CdM on PPAR-α was assessed and it was found that NK-CdM upregulated PPAR-α expression (Fig. 6D). Additionally, to evaluate the role of NK-CdM in UVB-induced lipid synthesis dysfunction, the mRNA expression levels of ELOVLs, CerSs, SPT2, SMS and ASM were examined. NK-CdM reversed the UVB-mediated downregulation of these genes (Fig. 6E-G). NK-CdM treatment restored the UVB-induced downregulation of CerS3, SPT and ASM protein expression (Fig. 6H).

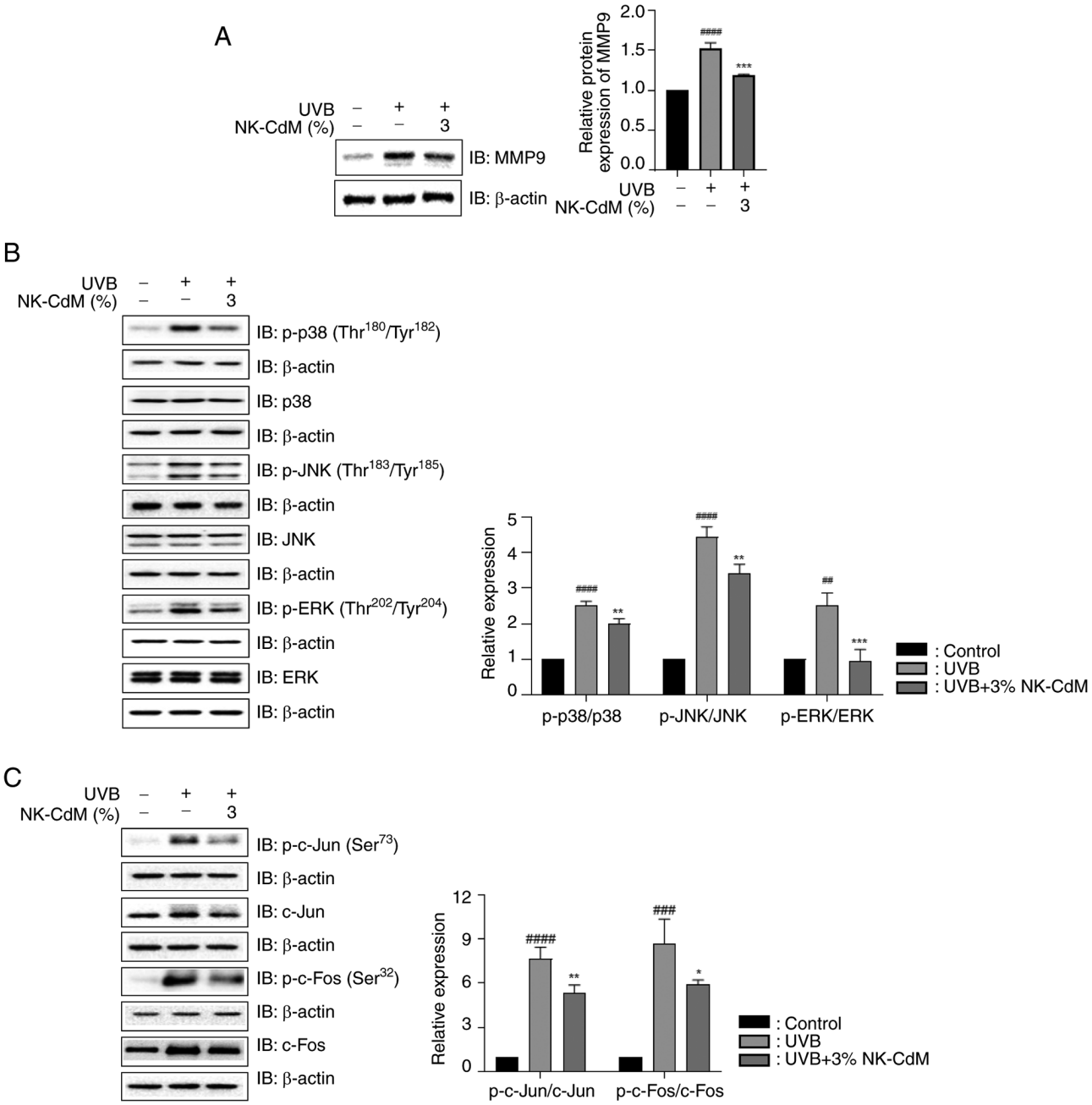

Figure 5. Effect of NK-CdM on the levels of MMP-9 and MAPK/AP-1 phosphorylation in UVB-stimulated HaCaT cells. Protein levels of (A) MMP-9; (B) p-p38 (Thr^{180}/Tyr^{182}), p-JNK (Thr^{183}/Tyr^{185}) and p-ERK (Thr^{202}/Tyr^{204}); (C) p-c-Jun (Ser^{73}) and p-c-Fos (Ser^{32}) were examined using western blot analysis. The results are expressed as the mean ± standard deviation of three independent experiment. $^{\#\#}$P<0.01, $^{\#\#\#}$P<0.001 and $^{\#\#\#\#}$P<0.0001 vs. the control group (untreated group). *P<0.05, **P<0.01 and ***P<0.001 vs. the UVB-irradiated group. The western blot results in (B) and (C) are images taken from different gels. NK-CdM, NK cell-conditioned medium; UVB, ultraviolet B; MMP, matrix metalloproteinase; p-, phosphorylated; JNK, c-Jun N-terminal kinases; ERK, extracellular signal-regulated kinase.

Discussion

With the increase in life expectancy, there is a growing concern for health and beauty, which has produced significant interest in the role of immune cells in skin health. The skin serves as a physical and chemical barrier and prevents moisture loss. Despite the unavoidable skin damage and aging caused by external factors, including UVR, cigarette smoke and other environmental pollutants, efforts are being made to mitigate these effects by enhancing the function of skin cells. In the present study, the effects of NK-CdM on UVB-induced skin photoaging were evaluated, demonstrating that NK-CdM effectively promotes the recovery of the skin barrier damaged by UVB exposure.

HA is naturally present in the epidermis, where it binds to the extracellular space via CD44 and may play a role in maintaining epidermal barrier function and hydration (23). HA synthesis is mediated by three types of HA synthases (HAS1, HAS2 and HAS3), which are localized to the inner plasma membrane (24). AQPs are membrane proteins that function as channels for water transport (25). Among them, AQP3 is the most abundant in the epidermis and is

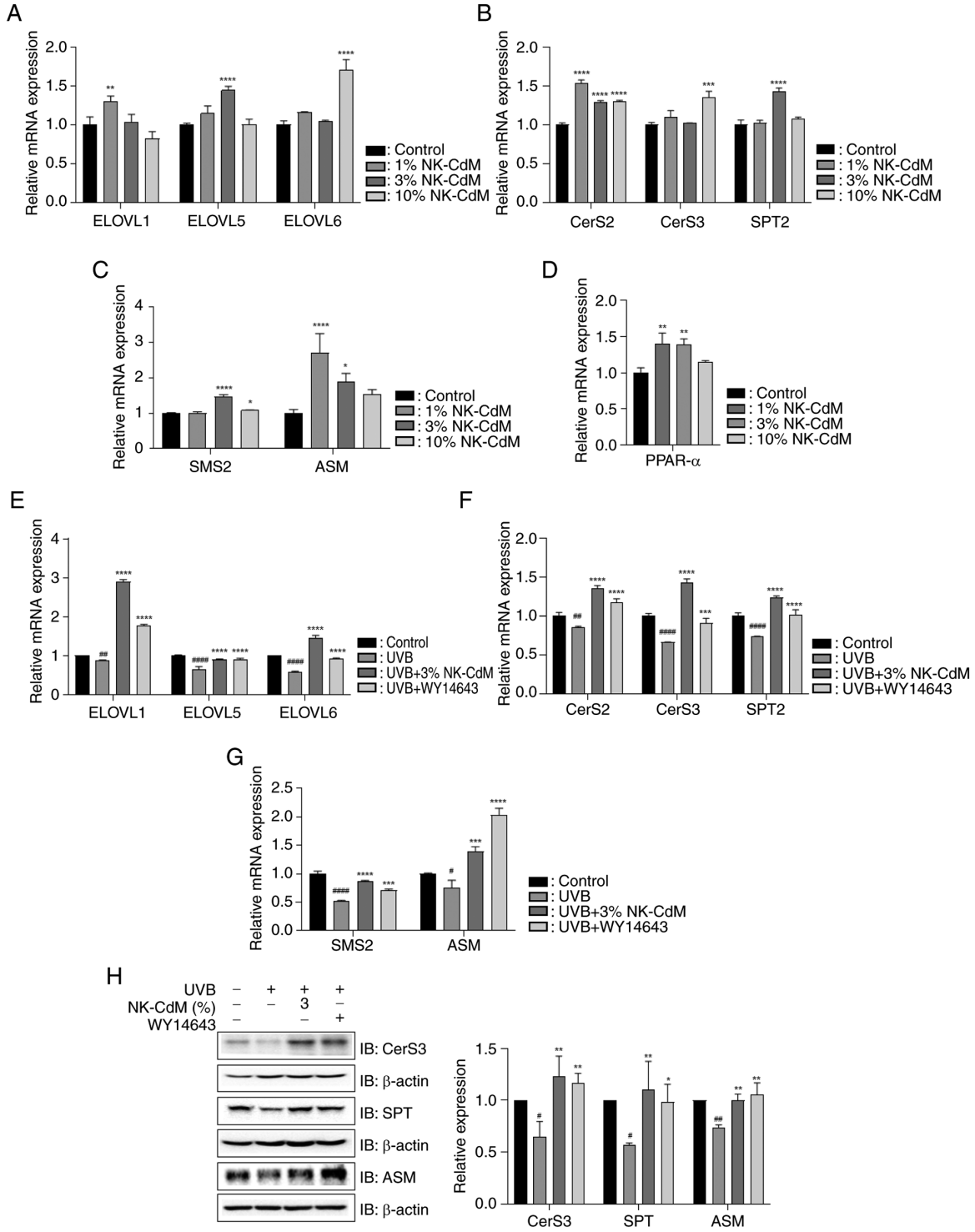

Figure 6. Effect of NK-CdM on skin lipid synthesis in UVB-stimulated HaCaT cells. Direct effect of NK-CdM on the mRNA levels of (A) ELOVL1, ELOVL5 and ELOVL6, (B) CerS2, CerS3 and SPT2, (C) SMS2 and ASM and (D) PPAR-α. The mRNA levels of (E) ELOVL1, ELOVL5 and ELOVL6, (F) CerS2, CerS3 and SPT2 and (G) SMS2 and ASM in HaCaT cells pretreated with 3% NK-CdM and WY14643 (1 μM) for 3 h, followed by UVB (30 mJ/cm^2) irradiation for 1 h. (H) The protein levels of CerS3, SPT and ASM were examined using western blotting (images taken from different gels). The results are expressed as the mean ± standard deviation of three independent experiment. $^{\#}$P<0.05, $^{\#\#}$P<0.01 and $^{\#\#\#\#}$P<0.0001 vs. the control group (untreated group). *P<0.05, **P<0.01, ***P<0.001 and ****P<0.0001 vs. the UVB-irradiated group. NK-CdM, NK cell-conditioned medium; UVB, ultraviolet B; ELOVL, elongation of very long chain fatty acids; CerS, ceramide synthases; SPT, serine-palmitoyl transferase; SMS, sphingomyelin synthase; ASM, acid sphingomyelinase.

crucial for skin hydration, as it transports both water and glycerol (26). Herein, NK-CdM preserved the mRNA and protein expression levels of HA1, HAS2, HAS3 and AQP3 under UVB irradiation conditions. In addition, NK-CdM prevented the reduction in HA production caused by UVB irradiation, indicating its crucial role in maintaining hydration homeostasis.

The free radical-oxidative stress theory of skin photoaging, extensively proposed by Sohal (27), suggests that oxidative stress plays a significant role in extrinsic skin aging,

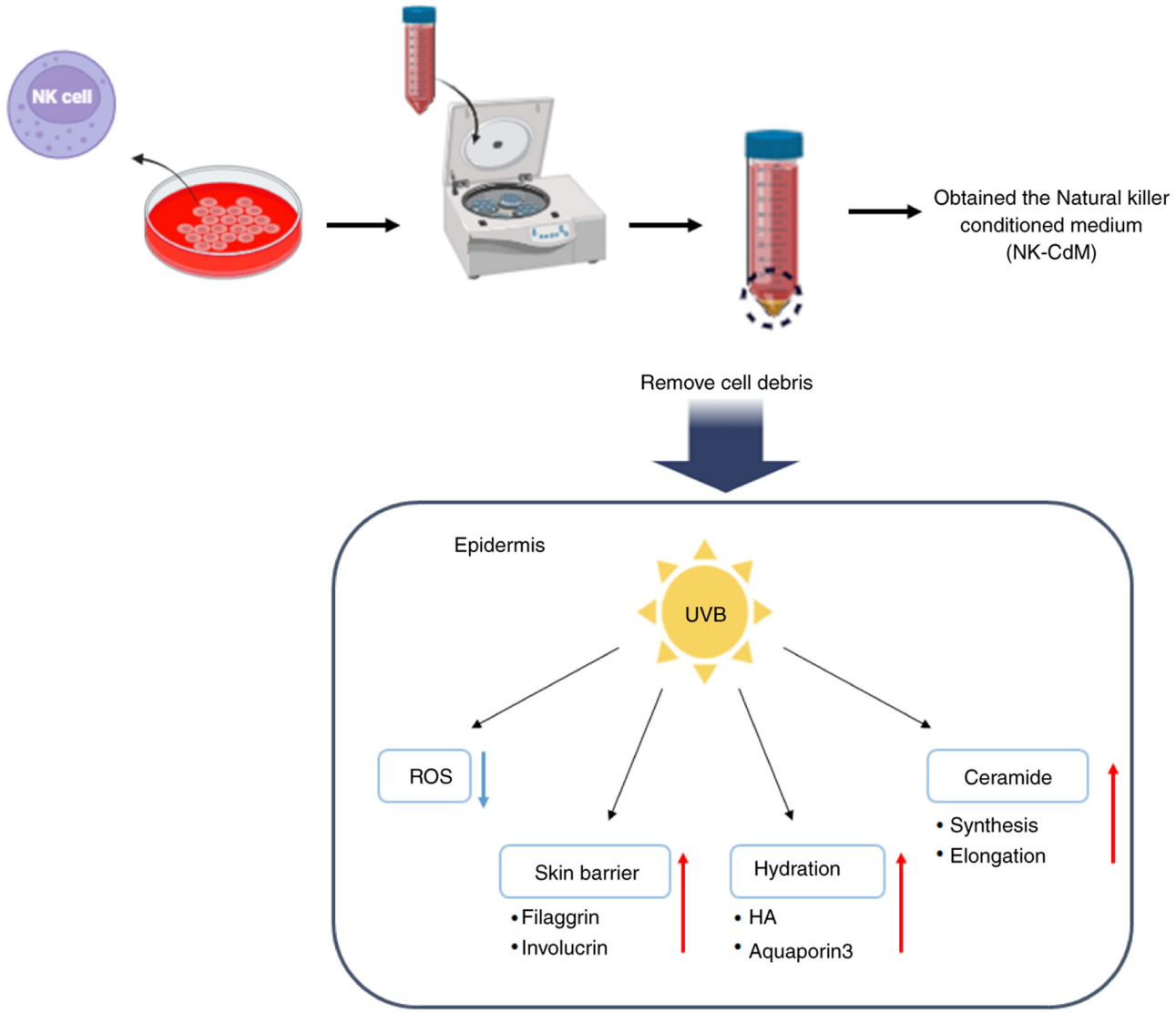

Figure 7. NK-CdM provides protection against photoaging caused by UVB exposure. Treatment with NK-CdM reduces ROS levels, improves skin barrier function by upregulating filaggrin and involucrin, enhances hydration via HA and aquaporin 3, and promotes ceramide synthesis and elongation. Consequently, NK-CdM plays a significant role in mitigating the adverse effects of UVB-induced photoaging. HA, hyaluronic acid.

with ROS being the major contributor (28,29). NK-CdM markedly suppressed ROS production, demonstrating its antioxidant properties. UVB-induced ROS activates MAPKs, culminating in the transcriptional regulation of MMPs and resulting in the degradation of collagen and elastin (30). In addition, AP-1, a heterodimer composed of proteins belonging to c-Fos and c-Jun, inhibits transforming growth factor β signaling, causing a reduction in collagen synthesis, subsequently leading to photoaging (31). NK-CdM suppressed UVB-induced MMP9 expression, MAPK expression and AP-1 activation. Therefore, it can be inferred that NK-CdM exhibits positive effects against UVB-induced photoaging.

Epidermal differentiation is the process in which keratinocytes in the epidermis undergo maturation (32). This process is crucial for maintaining skin health with several functions, including barrier, regulation of water balance, protection from UV radiation, immune response, regeneration and wound healing (33). The SC is the final product of the terminal differentiation of keratinocytes in the epidermis (34). In particular, FLG and IVL are essential proteins involved in the formation and functioning of the skin barrier, serving as important structural components in the SC (35). FLG primarily aids the organization and structural integrity of the SC and, upon proteolytic processing, produces free amino acids that contribute to natural moisturizing factors, helping to maintain skin hydration and pH balance (36). Conversely, involucrin provides mechanical strength and resilience to the skin (37). DPA promotes epidermal differentiation during the wound-healing process and increases skin hydration (38), thereby improving miniaturization and reducing transepidermal water loss, acting as an effective moisturizer. In HaCaT cells, NK-CdM demonstrated a more pronounced effect than DPA in inhibiting the reduction of FLG expression caused by UVB exposure. Furthermore, in the artificial skin model, IHC staining for FLG revealed that NK-CdM maintained FLG expression at a level comparable to that of DPA under UVB-exposed conditions. These findings suggested

that NK-CdM exhibits superior efficacy in protecting the skin barrier.

In the skin, cutaneous lipids contribute to the formation of an optimal epidermal barrier (39). CERs, which constitute ~50% of the intercellular lipid content, are particularly important (40). Alterations in the epidermal CERs content have been observed in certain inflammatory skin diseases, including atopic dermatitis (AD) (41). In AD skin lesions, the levels of CERs containing long-chain FAs (22-26 carbons in length) are markedly reduced, while CERs with short-chain FAs (<20 carbons in length) are elevated. This imbalance compromises the integrity of the skin barrier, leading to impaired function, increased water loss and decreased resistance to external irritants (42).

ELOVL elongases, particularly ELOVL-1, ELOVL-5 and ELOVL-6, are critical in the biosynthesis of CERs, as they elongate FAs to produce very long-chain fatty acids (VLCFAs) (43). These VLCFAs are essential components of CERs, which are crucial for maintaining the integrity and functionality of the skin barrier (44). The initial step in *de novo* sphingolipid synthesis, involving the condensation of serine and palmitoyl-CoA, is catalyzed by SPT (45). Ceramide synthases (CerS) 1 and 2 are key enzymes in the biosynthesis of CERs. Subsequently, SMS synthesizes sphingomyelin, while ASM hydrolyzes it between the SC and the stratum granulosum, ultimately producing CER in the SC, which forms a strong and cohesive lipid barrier (46,47). NK-CdM increases the expression levels of ELOVL-1, ELOVL-5 and ELOVL-6, as well as CerS-2 and CerS-3. It has been reported that the expression of PPAR-α is upregulated during epidermal differentiation. Activation of PPAR-α subsequently enhances the synthesis of cholesterol and CERs in keratinocytes (48,49). NK-CdM also increased the expression of PPAR-α, suggesting that NK-CdM not only stimulates epidermal differentiation but also promotes CER synthesis. Moreover, NK-CdM demonstrated a protective effect against the expression of CER synthesis-related factors induced by UVB, similar to the PPAR-α agonist WY14643.

The results of the present study demonstrated that NK-CdM effectively maintains and protects skin barrier homeostasis in HaCaT cells and 3D artificial skin exposed to UVB radiation (Fig. 7). However, there are major challenges that need to be addressed in future research. First, a larger, more diverse cohort is needed to improve the reproducibility and generalizability of the findings. In the future, the sample size will be increased to enhance the reproducibility and generalizability of the research findings. Second, there is currently no information on which specific cytokines within NK-CdM improve skin barrier damage caused by photoaging. Third, the study is limited by the inability to confirm the effects of NK-CdM on photoaging in a mouse model. Future research will aim to investigate the effects of NK-CdM in a mouse photoaging model. As a result, the effects of the designated NK-CdM medium cannot be scientifically substantiated at this time. Accordingly, future research will focus on identifying which cytokines included in NK-CdM are effective against photoaging.

In conclusion, these findings underscored the potential of NK-CdM for both cosmetic and therapeutic applications in mitigating UVB-induced skin aging.

Acknowledgements

Not applicable.

Funding

This research was supported by Basic Science Research Program through the National Research Foundation of Korea funded by the Ministry of Education (grant no. RS-2024-00349603).

Availability of data and materials

The data generated in the present study may be requested from the corresponding author.

Authors' contributions

JOL was responsible for the study conception and design, acquisition of data, analysis and interpretation of data, as well as drafting the manuscript or critically revising it for important intellectual content. JML was responsible for methodology, investigation, formal analysis, writing the manuscript and conduct of the experiments. YK and AYP were responsible for investigation, methodology and formal analysis. DY, SYK and JH were responsible for conducting the experiments and analysing the data. SH, HN, HS, KJ and MI were responsible for revising the manuscript and analysing the data. BJK was responsible for conceptualization, methodology, research and project administration. JOL and BK confirm the authenticity of all the raw data. All authors read and approved the final manuscript.

Ethics approval and consent to participate

Not applicable.

Patient consent for publication

Not applicable.

Competing interests

The authors declare that they have no competing interests.

References

1. Walker M: Human skin through the ages. Int J Pharm 622: 121850, 2022.
2. Zegarska B, Pietkun K, Zegarski W, Bolibok P, Wiśniewski M, Roszek K, Czarnecka J and Nowacki M: Air pollution, UV irradiation and skin carcinogenesis: What we know, where we stand and what is likely to happen in the future? Postepy Dermatol Alergol 34: 6-14, 2017.
3. Lotfollahi Z: The anatomy, physiology and function of all skin layers and the impact of ageing on the skin. Wound Pract Res 32: 6-10, 2024.
4. Baroni A, Buommino E, De Gregorio V, Ruocco E, Ruocco V and Wolf R: Structure and function of the epidermis related to barrier properties. Clin Dermatol 30: 257-262, 2012.
5. Wikramanayake TC, Stojadinovic O and Tomic-Canic M: Epidermal differentiation in barrier maintenance and wound healing. Adv Wound Care (New Rochelle) 3: 272-280, 2014.
6. Fisher GJ, Kang S, Varani J, Bata-Csorgo Z, Wan Y, Datta S and Voorhees JJ: Mechanisms of photoaging and chronological skin aging. Arch Dermatol 138: 1462-1470, 2002.

7. Ansary TM, Hossain MR, Kamiya K, Komine M and Ohtsuki M: Inflammatory molecules associated with ultraviolet radiation-mediated skin aging. Int J Mol Sci 22: 3974, 2021.
8. Brenner M and Hearing VJ: The protective role of melanin against UV damage in human skin. Photochem Photobiol 84: 539-549, 2008.
9. D'Orazio J, Jarrett S, Amaro-Ortiz A and Scott T: UV radiation and the skin. Int J Mol Sci 14: 12222-12248, 2013.
10. Tang X, Yang T, Yu D, Xiong H and Zhang S: Current insights and future perspectives of ultraviolet radiation (UV) exposure: Friends and foes to the skin and beyond the skin. Environ Int 185: 108535, 2024.
11. Rastogi RP, Richa Kumar A, Tyagi MB and Sinha RP: Molecular mechanisms of ultraviolet radiation-induced DNA damage and repair. J Nucleic Acids 2010: 592980, 2010.
12. Kozlov AV, Javadov S and Sommer N: Cellular ROS and antioxidants: Physiological and pathological role. Antioxidants (Basel) 13: 602, 2024.
13. Ngo V and Duennwald ML: Nrf2 and oxidative stress: A general overview of mechanisms and implications in human disease. Antioxidants (Basel) 11: 2345, 2022.
14. Lubos E, Loscalzo J and Handy DE: Glutathione peroxidase-1 in health and disease: From molecular mechanisms to therapeutic opportunities. Antioxid Redox Signal 15: 1957-1997, 2011.
15. Hammad M, Raftari M, Cesário R, Salma R, Godoy P, Emami SN and Haghdoost S: Roles of oxidative stress and Nrf2 signaling in pathogenic and non-pathogenic cells: A possible general mechanism of resistance to therapy. Antioxidants (Basel) 12: 1371, 2023.
16. Campbell KS and Hasegawa J: Natural killer cell biology: An update and future directions. J Allergy Clin Immunol 132: 536-544, 2013.
17. Lodoen MB and Lanier LL: Natural killer cells as an initial defense against pathogens. Curr Opin Immunol 18: 391-398, 2006.
18. Paul S and Lal G: The molecular mechanism of natural killer cells function and its importance in cancer immunotherapy. Front Immunol 8: 1124, 2017.
19. Kim DS, Kim DJ, Kim HP, Hwang SH and Kang JH: Potential of natural killer cell enriched conditioned media for skin care and anti-aging. J Cosmet Dermatol Sci Appl 11: 123-139, 2021.
20. Lee SE, Kwon TR, Kim JH, Lee BC, Oh CT, Im M, Hwang YK, Paik SH, Han S, Kim JY and Kim BJ: Anti-photoaging and anti-oxidative activities of natural killer cell conditioned medium following UV-B irradiation of human dermal fibroblasts and a reconstructed skin model. Int J Mol Med 44: 1641-1652, 2019.
21. Min B, Choi H, Her JH, Jung MY, Kim HJ, Jung MY, Lee EK, Cho SY, Hwang YK and Shin EC: Optimization of large-scale expansion and cryopreservation of human natural killer cells for anti-tumor therapy. Immune Netw 18: e31, 2018.
22. Livak KJ and Schmittgen TD: Analysis of relative gene expression data using real-time quantitative PCR and the 2(-Delta Delta C(T)) method. Methods 25: 402-408, 2001.
23. Kang MC, Yumnam S and Kim SY: Oral intake of collagen peptide attenuates ultraviolet B irradiation-induced skin dehydration in vivo by regulating hyaluronic acid synthesis. Int J Mol Sci 19: 3551, 2018.
24. Vigetti D, Genasetti A, Karousou E, Viola M, Clerici M, Bartolini B, Moretto P, De Luca G, Hascall VC and Passi A: Modulation of hyaluronan synthase activity in cellular membrane fractions. J Biol Chem 284: 30684-30694, 2009.
25. Agarwal S and Gupta A: Aquaporins: The renal water channels. Indian J Nephrol 18: 95-100, 2008.
26. Boury-Jamot M, Sougrat R, Tailhardat M, Le Varlet B, Bonté F, Dumas M and Verbavatz JM: Expression and function of aquaporins in human skin: Is aquaporin-3 just a glycerol transporter? Biochim Biophys Acta 1758: 1034-1042, 2006.
27. Sohal RS: Role of oxidative stress and protein oxidation in the aging process. Free Radic Biol Med 33: 37-44, 2002.
28. Chen X, Yang C and Jiang G: Research progress on skin photoaging and oxidative stress. Postepy Dermatol Alergol 38: 931-936, 2021.
29. Papaccio F, Arino A, Caputo S and Bellei B: Focus on the contribution of oxidative stress in skin aging. Antioxidants (Basel) 11: 1121, 2022.
30. Kim JM, Kim SY, Noh EM, Song HK, Lee GS, Kwon KB and Lee YR: Reversine inhibits MMP-1 and MMP-3 expressions by suppressing of ROS/MAPK/AP-1 activation in UV-stimulated human keratinocytes and dermal fibroblasts. Exp Dermatol 27: 298-301, 2018.
31. Silbiger S, Lei J and Neugarten J: Estradiol suppresses type I collagen synthesis in mesangial cells via activation of activator protein-1. Kidney Int 55: 1268-1276, 1999.
32. Moltrasio C, Romagnuolo M and Marzano AV: Epigenetic mechanisms of epidermal differentiation. Int J Mol Sci 23: 4874, 2022.
33. Meyer W and Seegers U: Basics of skin structure and function in elasmobranchs: A review. J Fish Biol 80: 1940-1967, 2012.
34. Haftek M, Oji V, Feldmeyer L, Hohl D, Hadj-Rabia S and Abdayem R: The fate of epidermal tight junctions in the stratum corneum: Their involvement in the regulation of desquamation and phenotypic expression of certain skin conditions. Int J Mol Sci 23: 7486, 2022.
35. Del Rosso JQ: Repair and maintenance of the epidermal barrier in patients diagnosed with atopic dermatitis: An evaluation of the components of a body wash-moisturizer skin care regimen directed at management of atopic skin. J Clin Aesthet Dermatol 4: 45-55, 2011.
36. McAleer MA, Jakasa I, Raj N, O'Donnell CPF, Lane ME, Rawlings AV, Voegeli R, McLean WHI, Kezic S and Irvine AD: Early-life regional and temporal variation in filaggrin-derived natural moisturizing factor, filaggrin-processing enzyme activity, corneocyte phenotypes and plasmin activity: Implications for atopic dermatitis. Br J Dermatol 179: 431-441, 2018.
37. Guneri D, Voegeli R, Gurgul SJ, Munday MR, Lane ME and Rawlings AV: A new approach to assess the effect of photodamage on corneocyte envelope maturity using combined hydrophobicity and mechanical fragility assays. Int J Cosmet Sci: Mar 23, 2018 (Epub ahead of print).
38. Camargo FB Jr, Gaspar LR and Maia Campos PM: Skin moisturizing effects of panthenol-based formulations. J Cosmet Sci 62: 361-370, 2011.
39. Knox S and O'Boyle NM: Skin lipids in health and disease: A review. Chem Phys Lipids 236: 105055, 2021.
40. Kono T, Miyachi Y and Kawashima M: Clinical significance of the water retention and barrier function-improving capabilities of ceramide-containing formulations: A qualitative review. J Dermatol 48: 1807-1816, 2021.
41. Upadhyay PR, Seminario-Vidal L, Abe B, Ghobadi C and Sims JT: Cytokines and epidermal lipid abnormalities in atopic dermatitis: A systematic review. Cells 12: 2793, 2023.
42. Janssens M, van Smeden J, Gooris GS, Bras W, Portale G, Caspers PJ, Vreeken RJ, Hankemeier T, Kezic S, Wolterbeek R, *et al*: Increase in short-chain ceramides correlates with an altered lipid organization and decreased barrier function in atopic eczema patients. J Lipid Res 53: 2755-2766, 2012.
43. Wang X, Yu H, Gao R, Liu M and Xie W: A comprehensive review of the family of very-long-chain fatty acid elongases: Structure, function, and implications in physiology and pathology. Eur J Med Res 28: 532, 2023.
44. Uchida Y: The role of fatty acid elongation in epidermal structure and function. Dermatoendocrinol 3: 65-69, 2011.
45. Hanada K: Serine palmitoyltransferase, a key enzyme of sphingolipid metabolism. Biochim Biophys Acta 1632: 16-30, 2003.
46. Jenkins RW, Canals D and Hannun YA: Roles and regulation of secretory and lysosomal acid sphingomyelinase. Cell Signal 21: 836-846, 2009.
47. Huh YE, Chiang MSR, Locascio JJ, Liao Z, Liu G, Choudhury K, Kuras YI, Tuncali I, Videnovic A, Hunt AL, *et al*: β-Glucocerebrosidase activity in GBA-linked Parkinson disease: The type of mutation matters. Neurology 95: e685-e696, 2020.
48. Chon SH, Tannahill R, Yao X, Southall MD and Pappas A: Keratinocyte differentiation and upregulation of ceramide synthesis induced by an oat lipid extract via the activation of PPAR pathways. Exp Dermatol 24: 290-295, 2015.
49. Rivier M, Castiel I, Safonova I, Ailhaud G and Michel S: Peroxisome proliferator-activated receptor-alpha enhances lipid metabolism in a skin equivalent model. J Invest Dermatol 114: 681-687, 2000.